

PAPER • OPEN ACCESS

## Online Monitoring of Overhead Power Lines Against Tree Intrusion via a Low-cost Camera and Mobile Edge Computing Approach

To cite this article: Peisong Li *et al* 2023 *J. Phys.: Conf. Ser.* **2422** 012018

View the [article online](#) for updates and enhancements.

You may also like

- [Overview of Energy Consumption Optimization in Mobile Edge Computing](#)  
Bingyi Hu, Jixun Gao, Yanxin Hu et al.
- [A survey of mobile edge computing in developing countries: challenges and prospects](#)  
O S Egwuche, M Ganiyu and M A Ibiyomi
- [Computation Offloading Based on Improved Glowworm Swarm Optimization Algorithm in Mobile Edge Computing](#)  
Ke Fu and Jun Ye

# Online Monitoring of Overhead Power Lines Against Tree Intrusion via a Low-cost Camera and Mobile Edge Computing Approach

Peisong Li<sup>1</sup>, Rui Qiu<sup>1</sup>, Minzhen Wang<sup>2</sup>, Xinheng Wang<sup>1\*</sup>, Shan Jaffry<sup>3</sup>, Ming Xu<sup>1</sup>, Kaizhu Huang<sup>4</sup> and Yi Huang<sup>5</sup>

<sup>1</sup> School of Advanced Technology, Xi'an Jiaotong-Liverpool University, Suzhou, 215123, China

<sup>2</sup> Changchun Institute of Technology, Changchun, 130012, China

<sup>3</sup> School of Internet of Things, Xi'an Jiaotong-Liverpool University, Suzhou, 215123, China

<sup>4</sup> Data Science Research Center & Division of Natural and Applied Sciences, Duke Kunshan University, Suzhou 215316, China

<sup>5</sup> Department of Electrical Engineering and Electronics, University of Liverpool, Liverpool, L69 3BX, UK

E-mail: \* [xinheng.wang@xjtlu.edu.cn](mailto:xinheng.wang@xjtlu.edu.cn)

**Abstract.** Fast-growing trees pose risks to the operational safety of overhead power lines. Traditional methods of inspecting tree growth, such as ground inspection, are time-consuming and not accurate. Latest development employs drones equipped with either light detection and ranging (LiDAR) or camera for accurate inspections. However, those methods are expensive and cannot be used all the time. They are also susceptible to severe weather conditions. Therefore, in this paper, an online method for measuring and calculating the horizontal distances between the power lines and trees in a mobile edge computing architecture is proposed by taking into account a unique property of power systems. Firstly, two-dimensional images are taken by a standard optical camera mounted on the tower. Secondly, the power lines and the surrounding trees in the images are discovered by processing the images. Finally, the distances between the power lines and trees are calculated based on a reference distance. Furthermore, the applications that control the cameras and image processing are implemented on a mobile edge server for real-time monitoring and system updates. Experiment results in real-world scenarios show that the measurement error is less than 10%, which indicates that the proposed approach can reliably estimate the distances and the edge computing-based architecture can improve the efficiency.

## 1. Introduction

The safety of power systems is jeopardized by fast-growing trees near overhead power lines. Flashovers can occur if the distance between trees and overhead lines is less than the prescriptive minimum safety range, resulting in short circuits of overhead lines [1]. Given the high financial expenses of power outages and the danger to people's lives from wildfires associated with power lines, it has become imperative for electric utility companies to monitor the trees to prevent unexpected intrusions [2].

Field survey or ground inspection is one of the conventional practices of tracking the tree status in which a team of linesmen is dispatched to visually evaluate the status of the overhead power lines via foot patrols and vehicle inspections. However, this method is costly because it



needs hiring of professional and well-trained staff. It is also time-demanding because it takes a certain period depending on the range of power networks. In addition, it is susceptible to observer's bias, weariness or a failure to detect invasion at the appropriate time. As a result, it may be difficult to determine whether the trees are intruding on the safe zone of power lines or not. Furthermore, severe weather conditions may hinder the inspection, and a delay in the inspection may result in the failure to discover fast-growing trees or damaged trees that are falling across power lines.

Recently, as shown in Fig. 1, Unmanned Aerial Vehicles (UAVs) equipped with Light Detection and Ranging (LiDAR) and various types of cameras are widely used in power line monitoring [3, 4, 5]. The abundant data resources ensure complete and accurate monitoring results. However, the use of UAVs for monitoring is still hampered by the fact that the operation relies heavily on the pilot's manual operation and his/her experience, which could threaten the safety of power systems and decrease inspection efficiency, if the operation was not taken appropriately [6].

In addition, due to limited battery supply, the UAVs can only fly for about half an hour after being powered up. The size of flying area is also limited due to the short communication range. Weather conditions may have an impact on the operation of UAVs as well. Under these constraints, the UAV-based technology cannot achieve a high detection frequency and the cost is prohibitive, which makes it unlikely that it will be widely adopted and implemented by electric utility companies.

In order to overcome the aforementioned problems, an image processing-based distance measurement methodology is proposed in this paper. Instead of employing UAVs, LiDAR, or labour and inspecting the power lines once a year or longer, a low-cost camera is mounted on the tower or the pole to take the images, as shown in Fig. 2. By using this method, power lines can be monitored continuously with minimal-to-no human involvement. In addition, the distances between trees and overhead power lines are calculated using a novel image processing method that takes into account the overhead power lines' distinctive characteristics. This approach is very easy to use, and the calculation is very efficient.

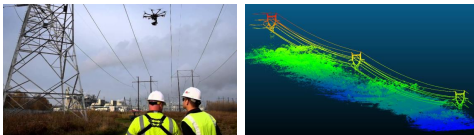


**Figure 1.** Power lines inspection using a LiDAR-mounted UAV

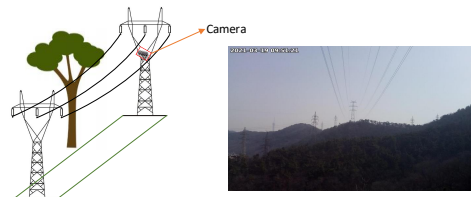


**Figure 2.** Illustration of monitoring the power lines using a camera

In order to support the real-time monitoring, reduce the burden of transmitting a large volume of images back to the control centre, and ensure a long-term reliable monitoring, a Mobile Edge Computing (MEC) architecture is implemented to ensure all the data is processed locally and only the calculated distances are normally transmitted back to the data centre. Owing to the use of the MEC architecture, images taken by the cameras, if needed for manual inspection, can be transmitted back to the control centre during the off-peak time to reduce the operation cost. Automatic monitoring and manual inspection of images ensure the reliability of the technology and safety of the power systems.

In addition, this MEC architecture also serves as a platform for future application customisation. Because edge servers are only responsible for cameras inside their territory, they have a considerable advantage in satisfying diversified requirements and interacting with

cameras based on the surrounding environmental information. Furthermore, flexibility is also a remarkable advantage of the MEC architecture and it is reflected in maintenance and expansion: When a single edge server is broken down, it has a considerably smaller impact than when cloud computing fails. The failed tasks can be transferred to other edge servers to maintain essential operations and the failed server can be replaced quickly without disrupting the normal operation of others; additionally, customized applications and computing resources could be deployed and allocated locally at the source of new demands when new tasks arise. Thus, this architecture lowers the long-term operation costs and enhances the monitoring efficiency of power lines.

For this paper, the main contributions are as follows:

(1) In order to solve the aforementioned problems caused by UAVs and LiDAR, only one ordinary optical camera is mounted on each tower to capture images and monitor the trees around power lines. This camera is low-cost and widely accessible, allowing for widespread deployment.

(2) In order to calculate the distances between trees and power lines from the collected images, one distinctive feature of the power systems is utilized, which lies in the fact that the physical distance between power lines is fixed and known. This fixed distance is used as a reference distance to determine other distances on the images, including the distances between the trees and lines.

(3) In order to support the real-time monitoring and reduce the burden of transmitting a large volume of images back to cloud, an MEC architecture was proposed. Rather than uploading all images to the cloud data center for processing, local processing is conducted at edge servers located nearby cameras. Only the processed distances are transmitted to the data center which significantly reduces the volume of the data and cost.

## 2. Related work

Nowadays, UAVs are becoming a cost-effective solution to observe power lines in close proximity. UAVs can be utilized as carriers to undertake thorough and accurate power line inspections when equipped with various remote sensing technologies such as optical cameras, LiDAR, infrared cameras, and ultraviolet cameras [7, 8, 3, 4, 5].

Optical cameras can be mounted on the UAV system to take images or videos. It has become the most extensively utilized device in UAV-based power line inspections due to its flexibility and high resolution [9].

Apart from the image-based approach, LiDAR is another widely applied technology in power line inspections that can produce point cloud to represent the 3D shape of the observed scene [10, 11].

Infrared thermal cameras and ultraviolet cameras are two other widely used UAV-carried remote sensing technologies for power line inspection. Matikainen et al. [12] reviewed the applications, especially the commercial uses, of infrared thermal cameras in power line monitoring. Kim et al. [13] proposed a smart inspection system that is mounted on UAV for power line inspection.

However, the primary impediment to the utilization of UAVs in power line inspections is the inability to continuously monitor the power lines. Another obstacle is the requirement of proficient skills to operate UAVs remotely in a complex and congested power line corridor [14, 15]. Therefore, the control of UAVs is usually executed manually or semi-automatically by pilots, which is costly and time-consuming.

In the last few years, Deep Learning-based technologies have made it possible to increase the accuracy of power line component identification in image-based inspections [16]. In [17], a high-voltage power lines monitoring system was developed by using consumer-grade UAVs equipped with a standard camera and a U-Net network for detecting vegetation encroachment. The U-Net is a kind of convolutional network designed for fast and precise image segmentation,

which has been applied in a variety of areas, including satellite imaging [18] and retina vessel segmentation [19]. Jenssen et al. [20] conducted a review on the latest literature and examined the existing vision-based power line inspection methods. After that, the potential of deep learning technologies for power line inspections was then concluded.

However, although such approaches are very promising, they rely heavily on the availability of abundant training data sets, and trained models can only be applied to new situations if the training sets are representative of the new situations.

Nowadays, LiDAR-based approaches are increasingly being adopted. In order to reduce reliance on UAV pilots and improve the inspection efficiency, Guan et al. [21] proposed an autonomous LiDAR-supported inspection concept and tested its feasibility. Nardinocchi et al. [22] proposed a 3-D Power Line Obstacle Detection (3-D-PowLOD) algorithm that first generates LiDAR point cloud and then separates power lines from the generated point cloud according to the fact that line points are isolated from other points. Pu et al. [23] designed a power line corridor inspection system using LiDAR and 4G communication for point clouds acquisition and results transmission, respectively. The main process includes decomposing tower components from sample data, separating cables from point clouds using a deep learning algorithm, recognizing potential risks based on the industry norms, and transmitting those risks in real time. Chen et al. [24] proposed a clearance measuring method, which extracts the power lines from LiDAR point clouds firstly and then calculates the minimal distance between lines and non-power-facility items. In [25], the location of power lines and surrounding vegetation can be estimated automatically based on the analysis of LiDAR point clouds. In this way, overgrowth vegetation can be monitored and removed in a timely manner and the risk of wildfire can be reduced.

LiDAR data can be used to create a precise 3D representation of an environment. However, collecting and processing LiDAR data are both expensive and time-consuming. If LiDAR-based power lines inspection is deployed for a large power transmission network, it is infrequent and needs once every one to two years to scan the entire area [26].

With the rise of satellite imagery data, it is now possible to monitor the vegetation continuously. Gazzea et al. [27] proposed to monitor the vegetation in the vicinity of power lines based on the analysis of satellite imagery employing a semi-supervised machine learning method. The stereo satellite imagery is utilized to measure the depth of trees in [28]. The proposed method has been shown to be more accurate than the block matching methodology.

Nowadays, MEC is introduced in power systems to construct the smart grid. In order to alleviate the pressure on central servers, Adeniran et al. [29] introduced edge computing architecture into power systems to construct smart grids. The design of the architecture takes into account resource allocation as well as the distribution of computing and communication burdens. Huang et al. [30] proposed to build edge computing-based smart grids, with a scheduling strategy and a heuristic algorithm incorporated to further reduce the delay and improve the frame rate. In [31], a smart grid application is designed so that the edge nodes and cloud can collaborate to boost processing rates. Experiments have revealed that the data processing rates can be increased to nearly 800k per second. Yang et al. [32] designed a smart grid network based on edge computing, which employs edge servers for task offloading and resource allocation. In this method, the cost can be drastically reduced while the delay remains unchanged.

However, it doesn't mean that MEC has already been completely implemented in power systems. These early research has laid down a perfect groundwork for implementing edge computing in power systems, but they are not completely equivalent to mobile edge computing. For traditional equipment, the calculation is limited to its pre-programmed programs, which is used to complete specific tasks.

The fact for monitoring trees is that the accuracy of the distance between the trees and

the power lines is not a critical parameter. A very accurate estimation is not quite a strict requirement. This inspires us to explore more cost-effective approaches to fulfill the task of maintaining the safety of the overhead lines. This paper demonstrates our new approach to do so.

### 3. Method

#### 3.1. Online monitoring methods

In this section, the distance calculation method between power lines and trees is introduced. The main problem to be solved is to find out the outermost line to the trees and distances between them are determined. Therefore, this method includes five steps: image edge detection, extraction of power lines, identification of outermost power lines, marking of warning areas, and distance calculation. The term "edge" is used both in image processing and mobile edge computing in this paper. In image processing, it means the boundary of two objects in the image; whilst in mobile edge computing, the edge means the position where computing is performed.

*3.1.1. Image Edge Detection* When the trees and power lines are taken in an image by the camera mounted on the tower, the first step is to identify the trees and power lines. Based on the nature of the work, only the edge of the trees facing the power lines is interesting to us. Thus the first step is to determine the edges in the image to find out the power lines and other obstacles that might pose a threat to the lines.

In this paper, the Sobel operator is used to perform edge detection for original images. On an image, the Sobel operator provides a 2D spatial gradient measurement. It's most commonly utilized to calculate an approximation of the gradient.

The operator calculates approximations of the derivatives using two  $3 \times 3$  kernels, as illustrated in Fig. 3, which are convolved with the original image to calculate horizontal and vertical changes, respectively. The calculation are as expressed in Eq. (1) and Eq. (2):

$$G_x = \begin{bmatrix} -1 & 0 & +1 \\ -2 & 0 & +2 \\ -1 & 0 & +1 \end{bmatrix} * A \quad (1)$$

$$G_y = \begin{bmatrix} +1 & +2 & +1 \\ 0 & 0 & 0 \\ -1 & -2 & -1 \end{bmatrix} * A \quad (2)$$

where  $A$  is defined as the original image, the initial point  $(0, 0)$  of the image is set at the top left,  $G_x$  and  $G_y$  are two images obtained by applying the horizontal and vertical mask on the original image, respectively. Then, the absolute gradient magnitude  $G$  at each point can be calculated by combining  $G_x$  and  $G_y$ . The calculation of  $G$  is shown in Eq. (3):

$$|G| = \sqrt{(G_x)^2 + (G_y)^2} \quad (3)$$

The process of edge detection is demonstrated in Fig. 4.

Edge detection produces a binary image as a result of its work. Binary images represent the images that only have two pixel values, typically expressed as 0 and 255, indicating black and white, respectively, where a threshold pixel is separating the pixels into either 0 or 255. Pixels with grey levels higher than the threshold are set to 255, while the rest are left at 0. In our case, the image after the edge detection is shown in Fig. 5.

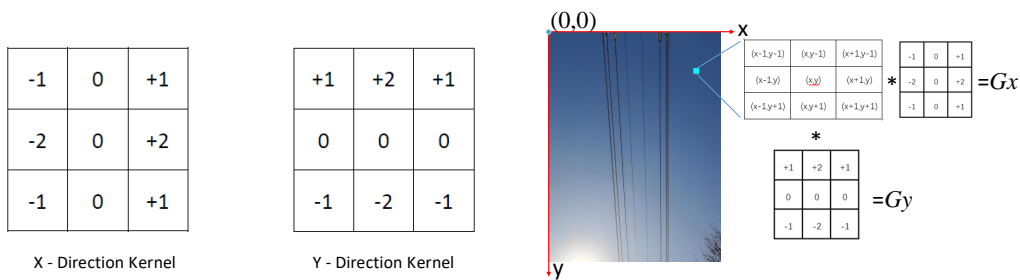


Figure 3. Sobel kernels

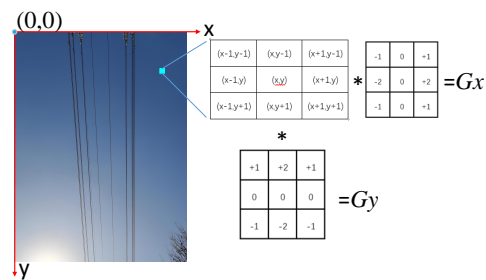


Figure 4. The process of edge detection

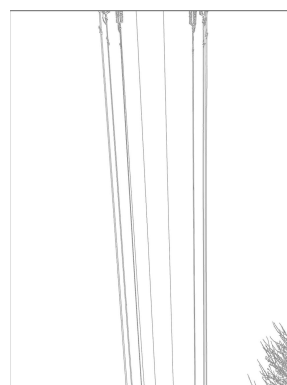


Figure 5. The binary image after edge detection

3.1.2. *Extraction of Power Lines* After edge detection, we need to extract the power lines from the binary image. The lines in the image could be described as a straight line. A straight line can be expressed as  $y = kx + b$  in a Cartesian coordinate system or as the form shown in Eq. (4) in a Polar coordinate system,

$$\rho = x * \cos\theta + y * \sin\theta \tag{4}$$

where  $\rho$  represents the shortest distance from the original point to the line,  $\theta$  represents the counter-clockwise angle produced by this shortest line and horizontal axis. The points on this line have same  $\rho$  and  $\theta$ .

Hough transform used in this paper is a technique for extracting characteristics of a specific shape in an image and that is typically used to recognize regular curves like lines or circles. We'll use the Polar system to represent lines for the Hough transform.

In one image, the coordinates of pixel point  $(x_i, y_i)$  are known variables, while  $\rho$  and  $\theta$  are unknown variables that need to be sought. Points in Cartesian image space can be converted to curves in the polar Hough parameter space when we plot the potential  $(\rho, \theta)$  values defined by each  $(x_i, y_i)$ . This process is shown in Fig. 6 and also called *point – to – curve* transformation. Points that are collinear in Cartesian image space become obvious when observed in Hough parameter space because all the converted curves are intersected at one point  $(\rho, \theta)$ .

The transform is carried out by quantizing the Hough parameter space into finite intervals or *accumulator cells*. When running the transform, each  $(x_i, y_i)$  is turned into a  $(\rho, \theta)$  curve, and the accumulator cells along this curve are increased. The resulting peaks in the accumulator array is a solid proof that a corresponding straight line exists in the original image.

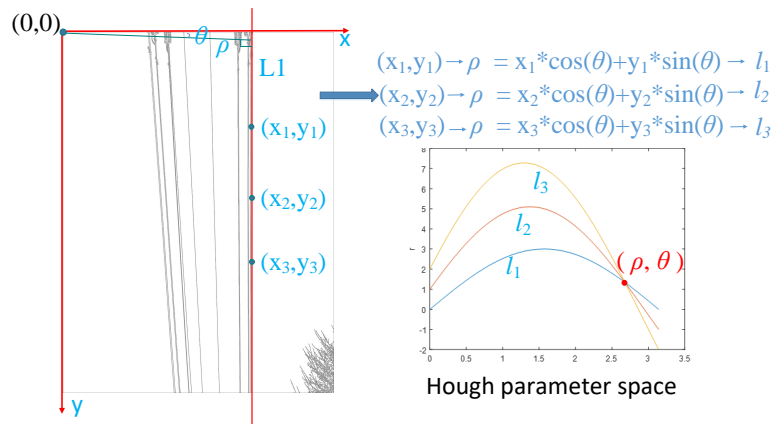


**Figure 6.** The process of Hough transform

*3.1.3. Identification of the Outermost Power Lines* Trees approach the outermost power line first when approaching a power line. The two outermost power lines must be identified in this scenario.

We know from Section 3.1.2 that each line detected by the Hough transform is represented by a vector  $(\rho, \theta)$ . Therefore, in order to identify the outermost power lines, the method we adopted is to calculate the perpendicular distance  $\rho$  to judge the two outermost lines in the image. Given the initial point  $(0, 0)$  is at the top left, the line with the smallest distance  $\rho$  in the image is the leftmost power line in the actual environment, while the line with the largest distance  $\rho$  is the rightmost power line in the actual environment. The calculation equations are listed in Eq.(5) and Eq.(6), respectively:

$$\rho_{min} = \min \{ \rho_1, \rho_2, \dots, \rho_n \} \tag{5}$$

$$\rho_{max} = \max \{ \rho_1, \rho_2, \dots, \rho_n \} \tag{6}$$

where  $n$  represents the total number of the recognized lines.  $\rho_{min}$  and  $\rho_{max}$  represent the leftmost line and rightmost line, respectively. The detected outermost power lines are shown in Fig. 7.

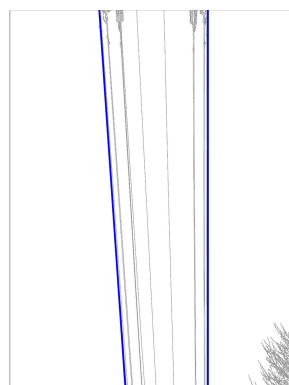


**Figure 7.** The detected outermost lines

*3.1.4. Marking of Warning Area* We need to mark the tree area when trees are overgrowing near power lines. We observed the gray value of the pixels on the left and right sides of the power lines in the binary image. If the gray value of a pixel is 0, it indicates that there is an object at this point. In order to avoid misidentification, in our design we do not treat pixels with a gray value of 0 as approaching trees right away. Instead, we set a threshold. When the number of pixels with a gray value of 0 on one side of the powerline exceeds this threshold, we assume that there is a high probability of having trees or other objects.

This process runs on the basis of the binary image obtained after edge detection. The dimensions of the image are  $w \times h$  pixels. Each pixel has a gray value of either 0 or 255. As shown in Fig. 8,  $L_l$  and  $L_r$  represent the leftmost and rightmost power lines, respectively. Starting from every pixel  $(x_i, y_i)$  on  $L_l$ , we traverse all the pixels on the left of this point and with the same vertical coordinate  $y_i$ , and count the number of pixel points with the gray value of 0. If the number is greater than the set threshold, in our case it is 20, it means that trees are likely to be close. Then the corresponding pixel  $(x_i, y_i)$  is marked; Similarly, for each pixel  $(x_j, y_j)$  on  $L_r$ , we traverse all the pixels on the right and with the same vertical coordinate  $y_j$ . If the number of the pixels with gray value of 0 is greater than a threshold, the pixel  $(x_j, y_j)$  is marked. This process and the marked warning area are shown in Fig. 8 and the corresponding pseudocode of this process is shown in Algorithm 1:

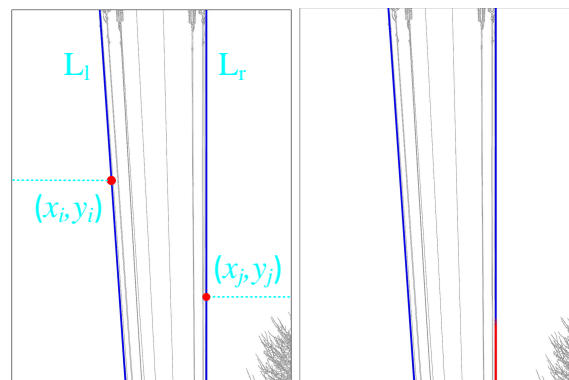


**Figure 8.** The process of marking warning area

*3.1.5. Distance Calculation* The warning area may be large, and the distances from the tree crowns to the power lines at different warning places may differ. Some branches (leaves) of tree crowns are very close to the power lines, and some are farther away. For safety reasons, we should mark the location of the branch (leaf) closest to the power line and measure this distance between the power line and the closest branch.

The method we adopted to detect the position of the shortest distance point is to calculate the ratio of the pixel distance between the tree crown and power line and the pixel distance between the two power lines. Since the tree crown and the power line are at the same height, the relationship they satisfied is shown in Eq. (7):

$$\frac{(d_p)_{y_i}}{(d_t)_{y_i}} = \frac{(D_p)_{y_i}}{(D_t)_{y_i}}, \quad y_i \in S \quad (7)$$

where  $d_p$  represents the pixel distance between power lines at  $y_i$  height in the image;  $d_t$  represents the pixel distance between the tree crown and line at the height of  $y_i$ ;  $D_p$  represents the physical distance between power lines;  $D_t$  represents the physical distance between the tree crown and

**Algorithm 1** Marking of warning area

---

**Input** : Initialization:  $w, h$   
**Output**: Marking of warning area  
 $threshold \leftarrow 20$ ;  
**for**  $i \leftarrow 1$  **to**  $h$  **do**  
     $count \leftarrow 0$ ;  
    **for**  $k \leftarrow 1$  **to**  $x_i$  **do**  
        **if**  $(k, y_i) = 255$  **then**  
             $count \leftarrow count + 1$ ;  
        **else**  
        **end**  
    **if**  $count \geq threshold$  **then**  
        The  $(x_i, y_i)$  is marked;  
    **else**  
**end**  
**for**  $j \leftarrow 1$  **to**  $h$  **do**  
     $count \leftarrow 0$ ;  
    **for**  $k \leftarrow x_j$  **to**  $w$  **do**  
        **if**  $(k, y_j) = 255$  **then**  
             $count \leftarrow count + 1$ ;  
        **else**  
        **end**  
    **if**  $count \geq threshold$  **then**  
        The  $(x_j, y_j)$  is marked;  
    **else**  
**end**  
**end**

---

power line, and  $S$  represents the warning area. The ratio of pixel distance between line-to-line pixel distance and tree crown-to-line pixel distance is equal to the ratio of the physical distance between them.

Therefore, the physical distance between the tree and power line can be obtained according to Eq. (8):

$$(D_t)_{y_i} = \frac{(d_t)_{y_i}}{(d_p)_{y_i}} \times (D_p)_{y_i}, \quad y_i \in S \quad (8)$$

As for the calculation of the physical distance between power line and tree crown, the actual physical distance  $D_p$  between two outermost power lines is fixed, because the installation of power lines is in accordance with the designed standards of power system. The value of  $D_p$  is a constant. Therefore, we can use this distance as a reference.

Then,  $d_t$  represents the pixel distance between  $(x_i, y_i)$  and the nearest pixel on the right and with a gray value of 0.

As shown in Eq. (8), in order to calculate  $D_t$ , we also need to measure the pixel distance  $d_p$  between the two outermost power lines in the image. As shown in Fig. 9, the lines corresponding to the two power lines in the image are not parallel, so the pixel distances between the two power lines at different heights in the image are different. Therefore, for each pixel  $(x_i, y_i)$  in the warning area  $S$  on the power line, we can calculate the value  $x_1$  of line  $L_l$  at height  $y_i$  and  $x_2$  of line  $L_r$  at height  $y_i$ , respectively. Then the pixel distance  $d_p$  between the two lines at height  $y_i$  can be obtained by Eq. (9):

$$d_p = |x_1 - x_2| \quad (9)$$

Since we need to measure the shortest physical distance  $(D_t)_{min}$  in the warning area,

according to Eq. (8), the shortest physical distance can be calculated by Eq. (10):

$$(D_t)_{min} = \min\left(\frac{d_t}{d_p} \times D_p\right) = \min\left(\frac{d_t}{d_p}\right) \times D_p \quad (10)$$

As can be seen from Eq. (10), the point in the warning area where the ratio of pixel distance between tree crowns and the closest line to pixel distance between lines is the smallest is the position where the shortest physical distance is located.

Finally, the shortest physical distance can be calculated according to Eq. (11):

$$(D_t)_{min} = \min\left(\frac{d_t}{d_p}\right) \times D_p = \frac{d_{min}}{|x_1 - x_2|} \times D_p \quad (11)$$

where  $d_{min}$  represents the shortest pixel length between tree crowns and power lines. The result is shown in Fig. 10.

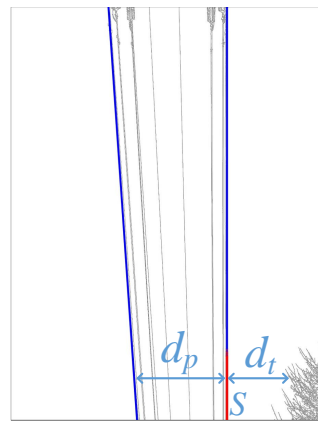


**Figure 9.** Looking for pixel position with the minimum distance

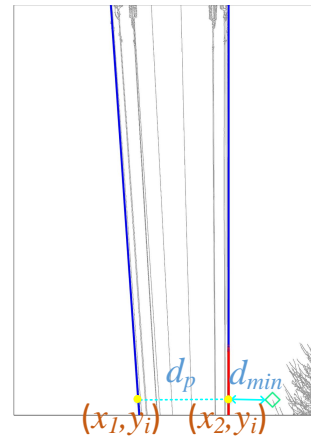


**Figure 10.** The Calculation of the shortest distance

### 3.2. Implementation of Edge computing

Currently, cloud computing is a generally acknowledged option for dealing with received data in power systems and utilities [33]. Cloud server can provide computation and storage services for the connected terminal devices. Nonetheless, this centralized cloud computing-based architecture may hinder utilities' future development. Firstly, cloud computing is limited by the limited bandwidth. Connecting millions of devices to the cloud may cause communication congestion and packet loss, as well as being technologically impossible. Secondly, the cloud might be overburdened, making it impossible to meet the diverse needs of thousands of devices. It's difficult to perceive and then analyze the heterogeneous data generated by various terminal devices, resulting in poor data analysis performance. Thirdly, cloud computing may undermine utility's data security. The risk of private or sensitive information being exposed increases when data is uploaded. In a word, cloud computing is not a panacea for all industrial applications.

In this section, an MEC-based power lines monitoring architecture was proposed, as illustrated in Fig. 11:

The architecture can be described as a three-layered structure: (1) Cloud layer, where the time-consuming tasks can be executed, the original images stored and the distance data

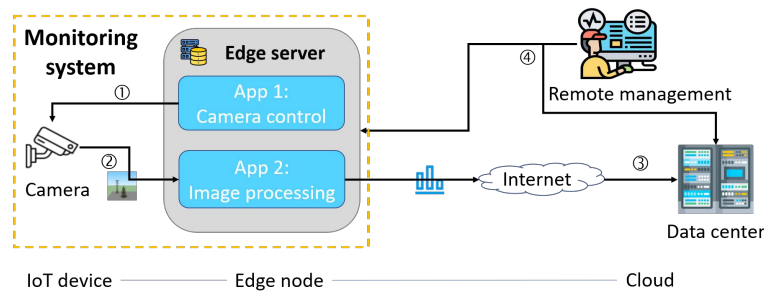


**Figure 11.** The architecture of the proposed powerlines monitoring system

measured; (2) Edge layer, which is made up of edge nodes that process the captured images and measure the distances before transmitting them to the Cloud; (3) IoT device layer, which is made up of cameras that capture images of power lines regularly and interact with edge nodes.

*3.2.1. Cloud Layer* The cloud server utilized in this project was purchased from *Tencent* and is situated in Beijing, it was adopted owing to its availability at our research facility and cost advantages over other cloud platforms [34].

The cloud layer serves as the controller of the monitoring system. It is responsible for receiving warning signals from all the edge nodes and reacting to those alerts according to the power utilities' policies. For example, if the cloud consistently receives warnings from a certain location, the power utilities will recognize that there is a potential hazard in that area and will proceed with the checking and restoration procedure.

*3.2.2. Edge Layer* The edge layer is made up of a group of edge nodes (servers), the edge node used in the system is Raspberry Pi, which is shown in Fig. 13. Each edge node is a fully functional Linux machine that runs dedicated applications. The edge layer is set up as an intermediate layer to communicate directly with the underlying devices as well as the upper cloud server on the *Tencent* platform. Depending on the network connectivity type, each edge server can connect to the Internet via WiFi or 5G.

One key application in this layer is the Image Processing Application (IP-App), which conducts the distance measuring algorithm based on the image processing model provided in Section 3. When the IP-App detects a threat in the received images, such as a tree growing too close to power lines, it uploads the measured data to the cloud along with warning information. Another key application is the Camera Control Application (CC-App). It controls the frequency at which the camera capture the images.

In addition, in the edge layer the applications are developed based on the container technology. Container technology has recently gotten a lot of attention [35]. It has the advantages of lightweight footprint and minimal overhead. The container can encapsulate a lightweight and portable package as a portable container image to run in any environment. In our project, each application and its required libraries are packaged into a container based on the container technology, which runs on the *Docker* platform, shared Host OS and underlying Infrastructure. *Docker* is a well-known platform for container standardization. The architecture of each edge node is shown in Fig. 12.

*3.2.3. IoT Device Layer* The IoT device layer is comprised of multiple terminal devices such as optical cameras used to monitor the power lines and trees. These devices are not only in charge of acquiring high-resolution images, but also equipped with a storage unit and a communication

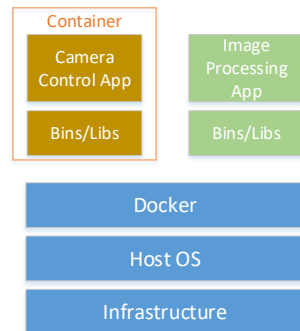


**Figure 12.** The structure of the containerized edge server



**Figure 13.** Raspberry Pi-based edge node

module for storing the images temporarily and transferring the processing results to the edge server, respectively.

## 4. Results

In this section, the performance and the effectiveness of the designed overhead power lines monitoring system are evaluated on both a simulated platform and a real world power system.

### 4.1. Simulation of The Test Scenario

In order to evaluate the proposed approach, a 3D model of the power line corridor is created using the 3D design software *SketchUp*. The camera is mounted on the tower as well as beneath the overhead power lines. The sketch map is shown in Fig. 14:

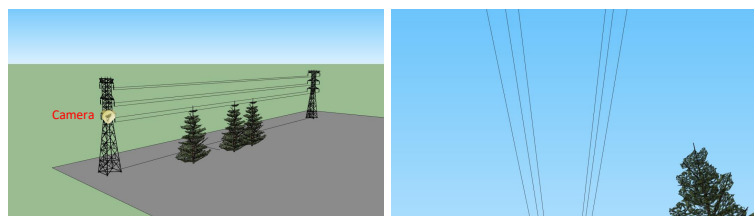


**Figure 14.** The 3D model of the power line corridor and the view of the camera

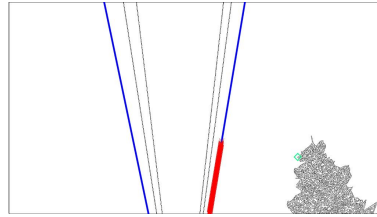
The inaccuracy rate, which is defined as the ratio of measurement error to actual distance, is used to evaluate the performance and accuracy of the proposed approach.

Fig. 15 shows the detection result after image processing and distance calculation, with the nearest point to the power lines highlighted in green. The calculated result is shown in Table 1.

In the 3D model, the actual physical distance between the two power lines is set to 10 meters. The actual minimal distance between power line and trees is 9 meters and the calculated distance between them is 9.6 meters. The inaccuracy rate is 6.7%, which is acceptable and demonstrates that the proposed approach can effectively monitor power lines.

### 4.2. Evaluation of the Power lines Monitoring Model

**4.2.1. On-site tests** After the 3D modeling and validation of the proposed method, we conducted an on-site experiment on a real power transmission system in Jiangsu Province,



**Figure 15.** The result after image processing and distance measurement

**Table 1.** The calculated result in simulation

| <b>Monitoring results</b>                     |       |
|---|-------|
| Physical distance between two outermost lines | 10 m  |
| Actual distance between line and tree         | 9 m   |
| Measured distance between line and tree       | 9.6 m |
| Inaccuracy rate                               | 6.7%  |

China. The monitoring system, as shown in Fig. 16, is comprised of one camera, a Raspberry Pi-based edge server and a 4G communication module.

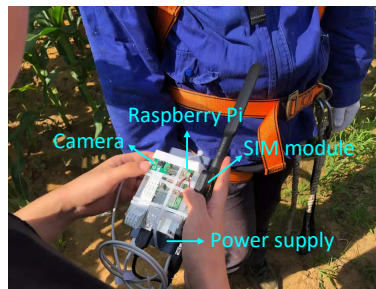


**Figure 16.** The integration of the monitoring system

Among them, the camera used in the experiment is Raspberry Pi Camera Module V2. The specific parameters are shown in Table 2:

**Table 2.** The parameters of the Camera Module V2

| <b>Parameters</b> | <b>Value</b>     |
|-------------------|------------------|
| Resolution        | 3280*2464 pixels |
| Sensor            | Sony IMX219      |
| Focal length      | 3.04mm           |
| Size              | 25*23*9mm        |

The Camera Control Application and the Image Processing Application run independently in the container and are deployed in the edge server. The parameters of the edge server are shown in Table 3:

**Table 3.** The parameters of the edge server

| Edge server    |  |
|----------------|--|
| Raspberry Pi 4 | 1.5GHz Quad-core Cortex-A72 (ARM v8)<br>8GB RAM<br>Gigabit Ethernet<br>Dual-band 2.4GHz/5GHz Wi-Fi |

*4.2.2. Tests of accuracy* In the experiment, the threshold of inaccuracy rate is set to 10%. Two images taken on different sites were chosen as examples and the results of image processing are shown in Fig. 17:

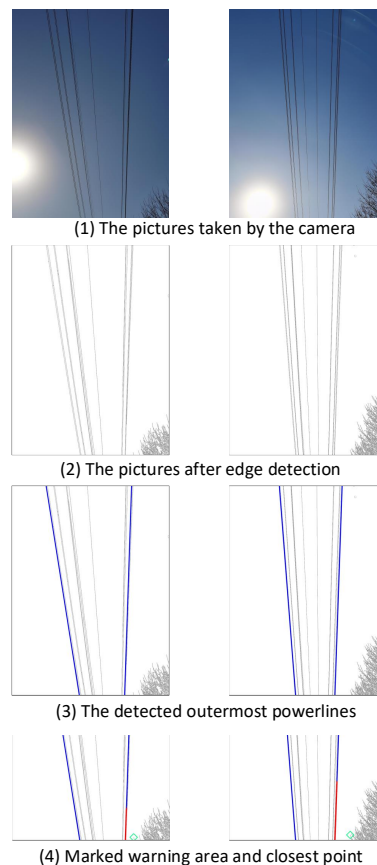
**Figure 17.** Step-by-step imaging processing of two pictures

Fig. 17 illustrates that the proposed method has achieved satisfactory measurement results: The two outermost power lines were extracted accurately using Hough transform. Then, the warning area and the site with the shortest distance are highlighted in the binary image. Next, the shortest distance between the power line and the closest tree crown is calculated according to Eq. (10). The calculation results are shown in Table 4:

As shown in Table 4, if there are trees close to the left or right side of the outermost power lines, the Image Processing Application can record the location of the nearest tree and then

**Table 4.** The calculated results

| Monitoring results                        | Image 1 |              | Image 2 |              |
|---|---------|--------------|---------|--------------|
|   | Left    | Right        | Left    | Right        |
| Pixel location of the nearest tree        | Null    | (2107, 3601) | Null    | (2099, 3559) |
| Pixel length between tree and line        |         | 143          |         | 262          |
| Pixel length between two outermost lines  |         | 799          |         | 693          |
| Calculated distance between line and tree |         | 43 cm        |         | 91 cm        |
| Actual distance                           |         | 46 cm        |         | 87 cm        |
| Inaccuracy rate                           |         | 6.5%         |         | 6.8%         |

calculate the shortest distance between the line and the nearest tree. The calculated distance is very close to the actual distance and the inaccuracy rate is acceptable (less than 10%), indicating that the proposed method is feasible for power lines monitoring. Furthermore, if the calculated distance falls below the safety threshold, the original captured image and the measured result will be uploaded to the cloud data center and will be double checked by maintenance staff. In order to demonstrate the benefits of the proposed method, we compared it to methods based on the Deep Learning algorithm [36], point cloud [37], and stereovision [38].

**Table 5.** Comparison with the state-of-the-art methods

| Method        | Year | Accuracy | Frequency | Cost          |
|---------------|------|----------|-----------|---------------|
| Deep Learning | 2021 | 87%      | Monthly   | \$250/km/year |
| Point cloud   | 2022 | 92.3%    | Monthly   | \$250/km/year |
| Stereovision  | 2020 | 96.64%   | Daily     | \$369         |
| Proposed      |      | 93.5%    | Daily     | \$100         |

The three most important factors in power line monitoring are detection accuracy, frequency, and cost. As shown in Table 5, the proposed method outperforms deep learning and point cloud algorithms for the detection accuracy of the distance between power lines and trees. Furthermore, because both deep learn-based and point cloud-based approaches require the assistance of UAVs, which is expensive and has a long inspection period. Whereas the proposed method just requires an optical camera, the proposed method also has clear benefits in terms of detection frequency and cost.

*4.2.3. Complexity analysis* The powerline inspection approach using UAV LiDAR takes 194 seconds to complete all the data processing procedures [9]. In contrast, the analysis and processing of each image, as well as the subsequent computation of the shortest distance, takes only around 30 seconds in our project. The computation time can be reduced by more than 80% with our strategy. This can be attributed to our proposed method's easy operation and uncomplicated computation.

## 5. Conclusion

In this paper, an overhead power lines monitoring system based on an edge computing architecture was proposed. In our method, the camera is mounted on each tower, and the Image Processing Application and the Camera Control Application are developed using container technology and deployed in an edge server using Edge computing architecture. The entire proposed system was tested in power systems on-site. The outermost power lines and the warning region in the image can be identified and highlighted by processing the images collected by cameras; then, after calculation, the location with the shortest distance in the image can be determined. The results of the tests demonstrate that the proposed model can measure the distance between power lines and trees accurately and quickly. Through the proposed method, electric utility companies can achieve continuous monitoring of power lines. When trees or other obstacles approach the power lines, this monitoring system can immediately detect and respond to it instantly, which considerably improves the safety of electrical networks. In addition, the employment of edge computing enables not only the easy maintenance and upgrade of the monitoring system, but also low cost of the operation by reducing the transmission of large volume of images.

## References

- [1] Kazim M, Khawaja A H, Zabit U and Huang Q 2019 *IEEE Transactions on instrumentation and measurement* **69** 2028–2038
- [2] Matikainen L, Lehtomäki M, Ahokas E, Hyypä J, Karjalainen M, Jaakkola A, Kukko A and Heinonen T 2016 *ISPRS Journal of Photogrammetry and Remote Sensing* **119** 10–31
- [3] Zhang Y, Yuan X, Fang Y and Chen S 2017 *ISPRS International Journal of Geo-Information* **6** 14
- [4] Hu Z, He T, Zeng Y, Luo X, Wang J, Huang S, Liang J, Sun Q, Xu H and Lin B 2018 *Protection and Control of Modern Power Systems* **3** 1–10
- [5] Oh J and Lee C 2017 *Sensors* **17** 2244
- [6] Guan H, Sun X, Su Y, Hu T, Wang H, Wang H, Peng C and Guo Q 2021 *International Journal of Electrical Power & Energy Systems* **130** 106987
- [7] Luo X, Zhang J, Cao X, Yan P and Li X 2014 *IEEE Transactions on Aerospace and Electronic Systems* **50** 1374–1389
- [8] Li Z, Liu Y, Walker R, Hayward R and Zhang J 2010 *Machine Vision and Applications* **21** 677–686
- [9] Oberweger M, Wendel A and Bischof H 2014 Visual recognition and fault detection for power line insulators *19th computer vision winter workshop* pp 1–8
- [10] Colomina I and Molina P 2014 *ISPRS Journal of photogrammetry and remote sensing* **92** 79–97
- [11] Yang L, Fan J, Liu Y, Li E, Peng J and Liang Z 2020 *IEEE Transactions on Instrumentation and Measurement* **69** 9350–9365
- [12] Matikainen L, Lehtomäki M, Ahokas E, Hyypä J, Karjalainen M, Jaakkola A, Kukko A and Heinonen T 2016 *ISPRS Journal of Photogrammetry and Remote sensing* **119** 10–31
- [13] Kim S, Kim D, Jeong S, Ham J W, Lee J K and Oh K Y 2020 *IEEE Access* **8** 149999–150009
- [14] Davies L, Bolam R C, Vagapov Y and Anuchin A 2018 Review of unmanned aircraft system technologies to enable beyond visual line of sight (bvlos) operations *2018 X International Conference on Electrical Power Drive Systems (ICEPDS) (IEEE)* pp 1–6
- [15] Azevedo F, Dias A, Almeida J, Oliveira A, Ferreira A, Santos T, Martins A and Silva E 2019 *Sensors* **19** 1812
- [16] Xie Q, Li D, Yu Z, Zhou J and Wang J 2019 *IEEE Transactions on Instrumentation and Measurement* **69** 5395–5406
- [17] Sikorska-Lukasiewicz K 2020 Methods of automatic vegetation encroachment detection for high voltage power lines *Radioelectronic Systems Conference 2019* vol 11442 (International Society for Optics and Photonics) p 114421G
- [18] Chhor G, Aramburu C B and Bougdal-Lambert I 2017 *Web: <http://cs229.stanford.edu/proj2017/final-reports/5243715.pdf>*
- [19] Jin Q, Meng Z, Pham T D, Chen Q, Wei L and Su R 2019 *Knowledge-Based Systems* **178** 149–162
- [20] Jenssen R, Roverso D *et al.* 2018 *International Journal of Electrical Power & Energy Systems* **99** 107–120
- [21] Guan H, Sun X, Su Y, Hu T, Wang H, Wang H, Peng C and Guo Q 2021 *International Journal of Electrical Power & Energy Systems* **130** 106987

- [22] Nardinocchi C, Balsi M and Esposito S 2020 *IEEE Transactions on Geoscience and Remote Sensing* **58** 8637–8648
- [23] Pu S, Xie L, Ji M, Zhao Y, Liu W, Wang L, Zhao Y, Yang F and Qiu D 2019 *Int. Arch. Photogramm. Remote Sens. Spat. Inf. Sci* **4213** 547–551
- [24] Chen C, Yang B, Song S, Peng X and Huang R 2018 *Remote Sensing* **10** 613
- [25] Takhirov S M and Israilov M S 2020 *Journal of Civil Structural Health Monitoring* **10** 947–956
- [26] McLaughlin R A 2006 *IEEE Geoscience and Remote Sensing Letters* **3** 222–226
- [27] Gazzea M, Pacevicius M, Dammann D O, Saponova A, Lunde T M and Arghandeh R 2021 *IEEE Transactions on Power Delivery*
- [28] Qayyum A, Malik A S, Saad M N M, Iqbal M, Ahmad R F, Abdullah T A R B T and Ramli A Q 2014 Monitoring of vegetation near power lines based on dynamic programming using satellite stereo images 2014 *IEEE International Conference on Smart Instrumentation, Measurement and Applications (ICSIMA)* (IEEE) pp 1–6
- [29] Adeniran A, Hasnat M A, Hosseinzadeh M, Khamfroush H and Rahnamay-Naeini M 2020 Edge layer design and optimization for smart grids 2020 *IEEE International Conference on Communications, Control, and Computing Technologies for Smart Grids (SmartGridComm)* (IEEE) pp 1–6
- [30] Huang Y, Lu Y, Wang F, Fan X, Liu J and Leung V C 2018 An edge computing framework for real-time monitoring in smart grid 2018 *IEEE International Conference on Industrial Internet (ICII)* (IEEE) pp 99–108
- [31] Carvalho O, Garcia M, Roloff E, Carreño E D and Navaux P O 2017 Iot workload distribution impact between edge and cloud computing in a smart grid application *Latin American High Performance Computing Conference* (Springer) pp 203–217
- [32] Yang C, Chen X, Liu Y, Zhong W and Xie S 2019 Efficient task offloading and resource allocation for edge computing-based smart grid networks *ICC 2019-2019 IEEE International Conference on Communications (ICC)* (IEEE) pp 1–6
- [33] Kulkarni N, Lalitha S and Deokar S A 2019 *International Journal of Electrical & Computer Engineering (2088-8708)* **9**
- [34] Chandel S, Ni T Y and Yang G 2018 Enterprise cloud: Its growth & security challenges in china 2018 *5th IEEE International Conference on Cyber Security and Cloud Computing (CSCloud)/2018 4th IEEE International Conference on Edge Computing and Scalable Cloud (EdgeCom)* (IEEE) pp 144–152
- [35] Huang Y, Cai K, Zong R and Mao Y 2019 Design and implementation of an edge computing platform architecture using docker and kubernetes for machine learning *Proceedings of the 3rd International Conference on High Performance Compilation, Computing and Communications* pp 29–32
- [36] Vemula S and Frye M 2021 Multi-head attention based transformers for vegetation encroachment over powerline corridors using uav 2021 *IEEE/AIAA 40th Digital Avionics Systems Conference (DASC)* (IEEE) pp 1–5
- [37] Chen Y, Lin J and Liao X 2022 *International Journal of Applied Earth Observation and Geoinformation* **108** 102740
- [38] Rong S and He L 2020 A joint faster rcnn and stereovision algorithm for vegetation encroachment detection in power line corridors 2020 *IEEE Power & Energy Society General Meeting (PESGM)* (IEEE) pp 1–5